

Optimization of Abrasive Powder Mixed EDM of Aluminum Matrix Composites with Multiple Responses Using Gray Relational Analysis

S. Singh and M.F Yeh

(Submitted July 21, 2010; in revised form December 14, 2010)

Abrasive powder-mixed electrical discharge machining (APM-EDM), a hybrid manufacturing process involving the use of a dielectric fluid mixed with abrasive powder, combines the benefits of mechanical and thermal interactions. The aim of this article is to use a new approach of performance evaluation, gray relational analysis (GRA), to evaluate the effectiveness of optimizing multiple performance characteristics of APM-EDM of 6061Al/Al₂O₃p/20p aluminum matrix composites (AMCs). The considered process parameter includes the seven control factors namely pulse current (A), pulse ON time (μs), duty cycle (%), gap voltage (V), time interval of tool lift (s), abrasive powder concentration (g/L), abrasive particle size (μm), and a noise factor, aspect ratio (shape of tool electrode). The combination of L18 (2¹ × 3⁷) orthogonal array design of experiment with GRA enables to determine the optimal parameters for multiple responses. GRA is used to obtain a single performance index, gray relational grade through gray relational coefficient to optimize the APM-EDM process with lower tool wear rate, surface roughness, and higher material removal rate. In addition, analysis of variance (ANOVA) for the GRC is also utilized.

Keywords AMCs, APM-EDM, gray relational analysis, multiple responses, optimization, orthogonal array

1. Introduction

Advanced materials, such as composites, super alloys, and ceramics, are “high-tech engineering materials” endowed with improved technological properties. They are key materials in industrial applications owing to their remarkable multiple functional characteristics such as improved strength, high hardness, low weight, and good thermal conductivity (Ref 1). Aluminum matrix composites (AMCs) refer to the class of lightweight, high-performance aluminum matrix material system reinforced with ceramic particulates (such as SiC, Al₂O₃, etc), which are highly potential material for many industries, including the aerospace, automobiles, defence, and recreation industries (Ref 2). According to Monaghan (Ref 3) and Boardman (Ref 4) their density is nearly one third that of steel, and offers high specific strength, stiffness, and superior wear resistance. AMCs often compete with super-alloys, ceramics, plastics, and re-designed steel parts in several aerospace and automotive applications (Ref 4). Singh et al.

reviewed that though near-net-shaped engineering components from AMCs are produced by Stir-casting method, but they do require frequent machining to achieve the desired dimensions and surface finish (Ref 5).

The widespread applications of AMCs are significantly impeded by their poor machinability and high machining costs with traditional machining methods such as turning, milling, drilling, etc., due to their reinforcement phase causing intrinsic brittleness, lower toughness, and ductility (Ref 6, 7). Müller and Monaghan (Ref 7) concluded that abrasive reinforcement results in poor stock removal, surface finish, and excessive tool wear by traditional machining methods. Review of past work reveals that electric discharge machining (EDM) is an effective non-traditional machining technique for the machining of AMCs, independent of their mechanical properties (Ref 6-8).

EDMed surface presents a matt finish due to a series of randomly laid tiny craters produced by the high-energy spark discharges and resolidification of debris from the craters, leading to formation of recast or white layer (Ref 5, 6). Furthermore, formation of heat-affected zone and micro-cracks causes metallurgical transformations of the work material. To increase the life of the EDMed components, the recast surface layer is removed by hand polishing, etching, burnishing, or shot peening, (Ref 9). Such supplementary finishing operations though refine the machined surface roughness (SR), but increase the production cost and manufacturing time. Hybrid manufacturing processes have come into existence due to continuous research and development in the field of non-traditional machining techniques.

Abrasive powder-mixed electrical discharge machining (APM-EDM) is one such hybrid process, which is firmly establishing its presence in effective machining of advanced materials with improved benefits.

S. Singh, Department of Mechanical Engineering, Sant Longowal Institute of Engineering and Technology (Deemed-to-be-University), Sangrur, Longowal, 148106 Punjab, India; and M.F Yeh, Department of Electrical Engineering, Lunghwa University of Science and Technology, Taoyuan, Taiwan, People's Republic of China. Contact e-mail: singh_shankar@yahoo.com.

1.1 APM-EDM

This process involves the use of abrasive powder such as SiC mixed into the dielectric fluid, resulting in good machinability and improved surface finish (Ref 10, 11). In this process, only one of the constituent processes, i.e., thermal interaction is directly involved in the material removal, while the mechanical interaction only assists in improving the machining capabilities by changing the operating conditions favorably (Ref 10). Furthermore, it has been found that the addition of powder widens the discharge gap thus decreasing the gap voltage and insulation strength of the dielectric fluid. The enlarged discharge passage also increases the discharge heat area and reduces the discharge density (Ref 12). This leads to the formation of evenly distributed, large diameter, and shallow craters, thus subsequently improving the surface finish (Ref 13).

Thus, APM-EDM greatly reduces the thermal stress and tendency to cracking. Examination of the machined surface of APM-EDMed workpieces reveals more uniform surface with less cracks, requiring no polishing or grinding to remove the resolidified layer, and can be utilized directly (Ref 10, 12, 13). The abrasive powder particles in the inter-electrode gap are energized due to the sonic waves generated under the sparking area. They do not follow a definite path, but instead behave in a zigzag fashion. The abrasive powder traveling in an angular direction creates a striking effect responsible for scooping of the work material and also dislodging of semi-conductive reinforcements when machining composites, whereas the one traveling in the straight direction are responsible for assisting in the formation of craters.

1.2 Mechanism of APM-EDM

In APM-EDM, aberration of electric field in the spark gap takes place due to the powder mixed dielectric, resulting in an increase in the inter-electrode gap. According to Zhao et al. (Ref 13), due to the applied gap voltage, the formation of positive and negative charges, respectively, at the top and bottom of the abrasive powders causes the “bridging effect” under the sparking area, creating multiple discharging effects within a single input pulse. Electric charges thus accumulated initiates discharge between the two consecutive powder particles, resulting in “series of discharges.” This can be explained with the help of Fig. 1 (Ref 5, 13). At points *a* and *b* on two adjacent powder particles, where the electric density is the highest, breakdown occurs when the field density surpasses the dielectric breakdown resistance. The electric discharge causes a short circuit between the two powder particles and redistribution of electric charges. Electric charges then accumulate at point's *c* and *d*, creating discharge between these two powder particles, and consequently leading to a “series of discharges” (Ref 13, 14). The powder particles due to bridging effect cause interlocking between the different powder particles and is displayed in the form of chain under the sparking area (Ref 15-22). This phenomenon increases the sparking intensity within a discharge leading to faster erosion from the work material surface and consequently the material removal rate (MRR) increases. Thus, electric discharge can easily occur in APM-EDM with enlarged spark gaps when compared to that in conventional EDM.

As seen in Fig. 2, the abrasive powder suspended in the dielectric fluid removes the material owing to the combined

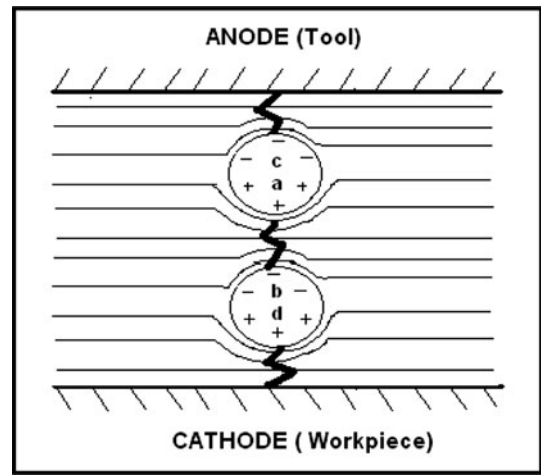


Fig. 1 Schematic diagram of “series of discharges” in APM-EDM (Ref 13, 14)

effect of mechanical thrust driven by the gas bubble explosion caused mainly from the working fluid evaporation and the striking impact of the suspended particles (Ref 23). This facilitates the removal of debris and other semi-conductive grains while machining composites, thus speeding up the discharge process. The mechanical interaction due to the striking effect helps in the dislodging of non-conductive Al_2O_3 particulates from the 6061 Al matrix, resulting in improved MRR. Thus, material removal of 6061 Al/ Al_2O_3 composite is attributed to the melting and evaporation of disintegrated Al matrix followed by the dislodging of Al_2O_3 grains.

2. Past Work

This section presents a brief summary of the review of the available literature on APM-EDM. Researches using kerosene as the dielectric fluid mixed with powder additive have been reported in the late 70s (Ref 24, 25). Jeswani (Ref 26) carried out some studies on the effects of the addition of graphite powders to kerosene dielectric fluid in EDM of mild steel work pieces using copper tools. An increase in the MRR (~60%), and a reduction in tool wear rate (TWR) (~15%) were reported. Narumiya et al. (Ref 15) investigated the effects of conductive powder suspended in working fluid on the EDM for finish machining of large workpieces. EDM characteristics studied with the aluminum, graphite, and silicon powder additives indicated that machining characteristics such as MRR and SR improved and better mirror-like machined surfaces were obtained (Ref 16). It has been suggested that addition of various powders in dielectric fluid during EDM results in improvement of performance measures in comparison to that achieved by conventional EDM (Ref 12).

Furutani et al. (Ref 17) reported a significant improvement in the machined surface properties, including wear resistance, hardness, and corrosion resistance using the powder mixed EDM process. It was reported that the gap distance between the tool electrode and the work material is increased from 25-50 to 50-150 μm .

It has also been observed by some researchers that the silicon powder material is dispersed into the work piece by a

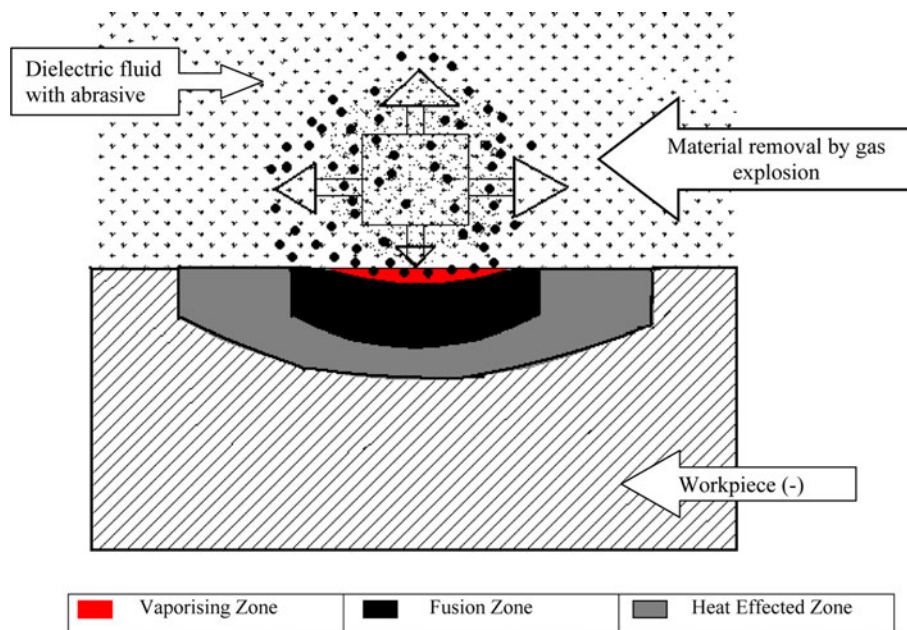


Fig. 2 Material removal by gas explosion during APM-EDM (Ref 23)

depth of several micrometers beneath the surface, thus improving the resistance of EDMed surface from corrosion and abrasion (Ref 18, 19). Investigations of powder mixed EDM on SKD 11 and Ti6Al-4V alloy with Al and SiC powders suspended in the dielectric fluid has also been reported (Ref 20). Tzeng and Lee (Ref 21) examined the discharge gap, MRR, and TWR, during machining of SKD 11 with copper electrode using pure kerosene and with kerosene-mixed with aluminum, chromium, copper, and SiC powder additives. Similarly, powder mixed EDM studies has also been conducted using various types of dielectric fluids, abrasive materials, grain size, grade, etc. (Ref 22, 27). The effects of impurities in the dielectric by mixing copper, aluminum, iron, and graphite powders in the dielectric fluid have also been reported (Ref 28).

Chow et al. (Ref 29) found an increase in the machining gap, and maximum machining rates were obtained with SiC powder whereas better surface finish is achieved with Al-mixed dielectric. Singh et al. performed ED machining of 6061 Al/Al₂O₃p/20P with copper tool electrode by mixing SiC powder into the dielectric fluid. Results indicated that TWR and SR decreased, whereas MRR increased significantly. However, the dimensional overcut was noticed to increase slightly during the abrasive EDM (Ref 11).

Zhao et al. suggested the “series of discharge,” which explains that the electric field intensifies due to powder additives in APM-EDM process (Ref 13). Chow et al. (Ref 29), on the other hand, suggested that a “multiple discharging effect” is created in APM-EDM process, caused by the dispersion of the discharge energy per single discharge pulse. However, both have reported that the powder additives mixed in the dielectric fluid facilitates the “bridging effect” and minimizes gap voltage and the insulating strength of the working media. The increase in powder concentration helps to bridge the gap between tool electrode and the work material, which results in the increased MRR.

Analysis of the past research shows that effects of a number of important APM-EDM machining parameters viz. electrode

lift time, aspect ratio (the tool electrode shape), abrasive particle size, and its concentration on the work material MRR and surface finish, obtained during the machining of AMCs, have not been addressed satisfactorily. The purpose of this study is to introduce the use of gray relational analysis (GRA) in selecting optimum APM-EDM conditions on multiple performance characteristics, namely, the MRR, TWR, and SR. To the best knowledge of the author of this study, published work evaluating the optimization and the effect of machining parameters on the multiple performance characteristics in APM-EDM of AMCs by using GRA have not been reported in referred journals.

In this study, an attempt has also been made to determine the most effective process parameter according to the order of importance (rating). In addition, optimal settings for APM-EDM machining parameters have been suggested.

3. Experimentation

3.1 Materials

Aluminum alloy (AA6061) was selected as the matrix material for this experiment. This alloy has liquidus and solidus temperatures of 650.8 and 582.8 °C, respectively. The alloy was reinforced with alumina (Al₂O₃) particulates (~20 μm). Plates of AA6061-based MMCs reinforced with 20% alumina (Al₂O₃) particulates were manufactured by one of the liquid metal processing technique known as Stir-casting method. 1% Mg and 2% Cu were also added to increase wettability and improve electrical conductivity of the composite material, respectively. The work material was molded into plates of 150 × 100 × 15 mm size. Electrolytic copper tool electrode (99.9%) having two different shapes viz. one square with aspect ratio 1.0 (size 40 × 40 mm) and other rectangular with aspect ratio 0.6 (size 24 × 40 mm), were used in this study. Machining

experiments for determining the optimal machining parameters were carried out based on design of experiments (DoE) and results analyzed via GRA.

3.2 DoE

In order to determine the effects of process parameters on the performance measures, all the experiments were planned based on DoE. The DoE methodology included the identification of control and noise factors of the APM-EDM process. Henceforth, in this study eight processing parameters were chosen, comprising seven control factors (C_1 - C_7 , viz. which can be controlled during experiments) at three levels each and one noise factor (N , viz. which cannot be controlled during experiments) at two levels. The specific levels were assigned on the basis of the preliminary experiments.

The control factors considered are pulse current, I_p (A), pulse ON time, T_{ON} (μ s), duty cycle, ζ (%), gap voltage, V_g (V), tool electrode lift time, T_L (s), abrasive powder concentration, APC (g/L), and abrasive particle size, APS (μ m) with three levels each, and a noise factor, aspect ratio viz, shape of the tool electrode (AR) at two levels. The responses considered are MRR (g/min), TWR (g/min), and SR, Ra (μ m). The factors and levels used in this experimentation are shown in Table 1.

The selection of the orthogonal array (OA) is based on the total degree of freedom of the process parameters. The degree of freedom, as defined, is the number of comparisons that needs to determine which level is better. The number of degrees of freedom associated with a factor is equal to one less than the number of levels for that factor (Ref 30). In this study, since there are seven control factors with three levels each, the degree of freedom is 14 [viz. $7 \times (3-1)$] and for one noise factor with two level it is one [2-1]. By neglecting the interaction among the process parameters in this study, the total degree of freedom is 15. The appropriate OA is selected on the basis of the condition that the degree of freedom for the OA should be greater than or equal to that of the process parameters. Therefore, a mixed-level orthogonal array design $L18$ ($2^1 \times 3^7$) comprising eighteen rows and eight columns was selected for this study to accommodate one noise factor (two level) and seven control factors (three levels each). The outer array was chosen to be the aspect ratio (i.e., noise factor).

3.3 Experimental Details

An electric discharge machine (E-ZNC) (Make: Electronica), powered by a PS-50 generator, max^m. working current 50 A and X, Y, Z, traverses as 300, 200, and 250 mm, respectively, was used as the experimental machine in this study, by incorporating a modified dielectric fluid circulation system for dielectric and abrasive powder/dielectric mixture. Spark erosion

oil (SEO-250; flash point 94 °C, make: IPOL) was used as dielectric fluid for the experiments. In the dielectric fluid, solid SiC abrasive powder having different grain sizes and concentrations were mixed to perform APM-EDM experiments. In order to ensure proper mixing of the abrasive powder with the dielectric fluid, a mechanical stirrer was also incorporated into the system. The filter system for recirculation of the dielectric medium was specifically designed to filter out the work material debris, whereas the powders are re-circulated during the experiment for reuse (Ref 5, 21). The schematic diagram of the modified dielectric/powder supply system for APM-EDM is shown in Fig. 3 (Ref 22, 31, 32).

The experiments were carried out using $L18$ ($2^1 \times 3^7$) OA, an un-replicated full-factorial experimental design, with a run size of 18, to determine the optimal parameter settings. The experimental layout of $L18$ for the experimental parameters is shown in Table 2. The machining parameters such as I_p (A), T_{ON} (μ s), ζ (%), V_g (V), and T_L (s) were controlled by the machine itself after setup, since being machine settings. Each run was repeated three times. MRR (g/min) and TWR (g/min) for each run were calculated on the basis of weight difference before and after machining using a Sartorius E-1200S precision scale (max. capacity-1210 g and precision accuracy of 0.01 mg). A Taylor-Hobson SR tester was used to measure SR, Ra with an accuracy of 0.1 μ m. The APM-EDM experimental results are listed in Table 3.

4. Analysis Method

4.1 Gray System Theory (GST)

The GST was first proposed many decades ago but has been extensively applied only since the last decade. GST, a developed system engineering theory based on the uncertainty of small samples, was initiated by Deng (Ref 33) in P.R. China. GST gradually developed from requirements for new methods to solve certain problems for solving the complicated inter-relationships among the multiple performance characteristics. The system was named using “gray” as the color, which indicates the amount of known information in control theory. Infact “gray” implies poor, incomplete, and uncertain, and is especially used in relation to the concept of information. In system control theory, a system for which the relevant information is completely known is a “white” system, while a system for which the relevant information is completely unknown is termed a “black” system. Any system between these limits then may be called a gray system and provides an approach for abstract modelling of systems for which the

Table 1 Factors and their levels

| Factor | Experimental parameters | Symbol, units | Level 1 | Level 2 | Level 3 |
|--------|-------------------------------|--------------------|---------|---------|---------|
| A | Aspect ratio | AR | 0.6 | 1.0 | ... |
| B | Pulse current | I_p , A | 10 | 15 | 20 |
| C | Pulse ON time | T_{ON} , μ s | 50 | 100 | 200 |
| D | Duty cycle | ζ , % | 0.4 | 0.5 | 0.7 |
| E | Gap voltage | V_g , V | 40 | 45 | 50 |
| F | Tool electrode lift time | T_L , s | 2.0 | 3.0 | 5.0 |
| G | Abrasive powder concentration | APC, g/L | 8 | 10 | 12 |
| H | Abrasive particle size | APS, μ m | 74 | 45 | 37 |

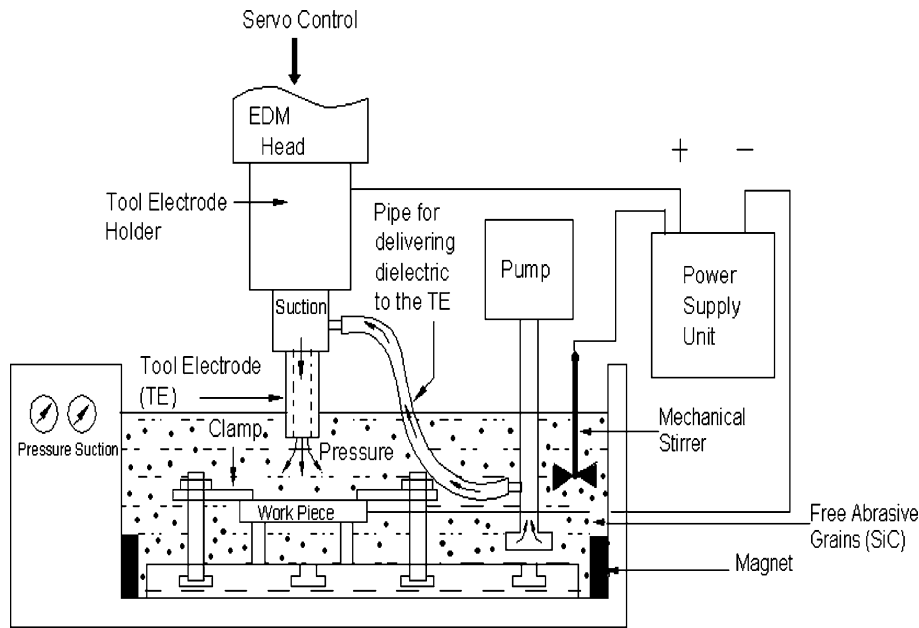


Fig. 3 Schematic diagram of the modified AEDM system on E-ZNC machine

Table 2 Experimental layout using a L18 ($2^1 \times 3^7$) orthogonal array

| No. of run/factor | N | C ₁ | C ₂ | C ₃ | C ₄ | C ₅ | C ₆ | C ₇ |
|-------------------|---|----------------|----------------|----------------|----------------|----------------|----------------|----------------|
| 1 | 1 | 1 | 1 | 1 | 1 | 1 | 1 | 1 |
| 2 | 1 | 1 | 2 | 2 | 2 | 2 | 2 | 2 |
| 3 | 1 | 1 | 3 | 3 | 3 | 3 | 3 | 3 |
| 4 | 1 | 2 | 1 | 1 | 2 | 2 | 3 | 3 |
| 5 | 1 | 2 | 2 | 2 | 3 | 3 | 1 | 1 |
| 6 | 1 | 2 | 3 | 3 | 1 | 1 | 2 | 2 |
| 7 | 1 | 3 | 1 | 2 | 1 | 3 | 2 | 3 |
| 8 | 1 | 3 | 2 | 3 | 2 | 1 | 3 | 1 |
| 9 | 1 | 3 | 3 | 1 | 3 | 2 | 1 | 2 |
| 10 | 2 | 1 | 1 | 3 | 3 | 2 | 2 | 1 |
| 11 | 2 | 1 | 2 | 1 | 1 | 3 | 3 | 2 |
| 12 | 2 | 1 | 3 | 2 | 2 | 1 | 1 | 3 |
| 13 | 2 | 2 | 1 | 2 | 3 | 1 | 3 | 2 |
| 14 | 2 | 2 | 2 | 3 | 1 | 2 | 1 | 3 |
| 15 | 2 | 2 | 3 | 1 | 2 | 3 | 2 | 1 |
| 16 | 2 | 3 | 1 | 3 | 2 | 3 | 1 | 2 |
| 17 | 2 | 3 | 2 | 1 | 3 | 1 | 2 | 3 |
| 18 | 2 | 3 | 3 | 2 | 1 | 2 | 3 | 1 |

information is limited, incomplete and characterized by random uncertainty (Ref 34).

The main gray methods within GST are (gray) systems and control, gray modelling (GM), and GRA (Ref 35, 36). GRA is used for system analysis, as an alternative for classical statistical methods, and has been exploited by many scientists in different areas including medicines (Ref 35, 37-50). GRA uses the gray relational coefficient (GRC) to describe the trend relationship between an objective series and a reference series at a given point in a system. For a given reference sequence and a given set of comparative sequences, GRA can be used to determine the gray relational grade (GRG) between the reference and each comparative sequence in the given set.

On further analyses, best comparative one can be found by the resultant GRGs. The analysis by classical statistical procedures may not be acceptable without large data sets and data satisfying certain mathematical criteria. The GST, on the contrary, makes use of relatively small data sets, less duration, and does not demand strict compliance to certain statistical laws, simple or linear relationships among the observable (Ref 39). The classical techniques are often unable to satisfy the requests for multiple performance characteristics optimization, due to the demand for the large measured values, which becomes inconvenient to acquire (Ref 41, 42, 45). The original Taguchi Method, one of the DoE techniques, is capable to optimize a single performance characteristic (Ref 42, 45). Handling the optimization of multiple performance characteristics is an interesting research field, and resolved by GRA.

4.2 GRA

It is a normalization-based evaluation technique, requiring a sample of only limited (*generally insufficient from a statistics point of view*) size, of discrete sequential (time-series) data to enable reliable modelling and estimation of system behavior (Ref 39). Furthermore, statistical methods require a probability distribution for the values in the evaluation matrix. In some cases, a probability distribution cannot be determined due to, for instance, limited availability of data. GRA does not require such probability distribution.

In GRA, it is assumed that the input attributes satisfy three conditions for comparability of the set of series: (1) for each attribute vector the difference between the maximum and the minimum input values is less than an order of magnitude of two; (2) all attributes in an attribute vector are of the same type (maximum value, minimum value, or optimum value); and (3) all attributes in an attribute vector have the same measurement scale, and, if in a quantitative scale, have the same unit or no unit (Ref 33). Accordingly, in GRA literature these conditions are referred to as scaling (for the order of magnitude), polarization (for the attribute type), and non-dimension

Table 3 Experimental results obtained for MRR, TWR, and SR

| No. of run | MRR, g/min | | | TWR, g/min | | | SR, Ra, μm | | |
|------------|------------|------|------|------------|--------|--------|------------|------|------|
| | 1 | 2 | 3 | 1 | 2 | 3 | 1 | 2 | 3 |
| 1 | 0.38 | 0.44 | 0.37 | 0.0094 | 0.0099 | 0.0098 | 2.77 | 2.8 | 2.23 |
| 2 | 0.36 | 0.39 | 0.34 | 0.0101 | 0.0104 | 0.0104 | 3.59 | 2.61 | 2.65 |
| 3 | 0.34 | 0.28 | 0.36 | 0.0122 | 0.0121 | 0.0126 | 3.56 | 4.3 | 3.84 |
| 4 | 0.47 | 0.36 | 0.42 | 0.0090 | 0.0091 | 0.0092 | 4.21 | 3.77 | 3.52 |
| 5 | 0.47 | 0.51 | 0.48 | 0.0094 | 0.0095 | 0.0090 | 3.0 | 4.1 | 3.1 |
| 6 | 0.53 | 0.39 | 0.52 | 0.0114 | 0.0118 | 0.0116 | 4.3 | 4.18 | 4.42 |
| 7 | 0.41 | 0.46 | 0.42 | 0.0101 | 0.0103 | 0.0102 | 3.56 | 3.31 | 2.76 |
| 8 | 0.52 | 0.42 | 0.55 | 0.0129 | 0.0130 | 0.0134 | 3.03 | 2.61 | 3.66 |
| 9 | 0.34 | 0.46 | 0.51 | 0.0148 | 0.0149 | 0.0141 | 4.18 | 3.9 | 4.52 |
| 10 | 0.38 | 0.37 | 0.49 | 0.0100 | 0.0105 | 0.0101 | 3.96 | 3.91 | 4.13 |
| 11 | 0.39 | 0.34 | 0.49 | 0.0123 | 0.0127 | 0.0122 | 4.09 | 4.59 | 5.12 |
| 12 | 0.54 | 0.48 | 0.36 | 0.0104 | 0.0104 | 0.0101 | 2.97 | 2.83 | 2.3 |
| 13 | 0.29 | 0.31 | 0.33 | 0.0073 | 0.0079 | 0.0080 | 2.69 | 2.25 | 2.82 |
| 14 | 0.38 | 0.45 | 0.4 | 0.0138 | 0.0137 | 0.0142 | 4.99 | 4.4 | 4.41 |
| 15 | 0.57 | 0.54 | 0.65 | 0.0128 | 0.0120 | 0.0121 | 2.72 | 3.91 | 2.37 |
| 16 | 0.51 | 0.42 | 0.32 | 0.0117 | 0.0120 | 0.0117 | 2.34 | 2.9 | 3.22 |
| 17 | 0.46 | 0.49 | 0.47 | 0.0122 | 0.0127 | 0.0120 | 3.29 | 2.6 | 3.43 |
| 18 | 0.44 | 0.49 | 0.54 | 0.0124 | 0.0129 | 0.0139 | 4.4 | 4.9 | 3.6 |

(for the measurement scale). If these three conditions are not satisfied, normalization of the input data prior to GRA processing is required. By applying normalization (i.e., the data pre-processing), compliance with the three conditions is achieved.

Before calculating the GRG, we must perform data pre-processing (normalizing in the range between zero and unity). This step is called “gray relational generating” (Ref 51). Normalizing involves transferring the original sequence to a comparable sequence. Depending on the characteristics of a data sequence, there are various method-ologies of data pre-processing available for the GRA (Ref 52). Therefore, the series data can be treated with the following three situations and the linearity of normalization to avoid distorting the normalized data (Ref 53). After normalization the reference series is identified. In this study, normalization of the experimental results obtained for MRR, TWR, and SR were performed, in the range between 0 (black) and 1 (white).

The experimental results are tabulated in Table 3. In general, for a maximum value-type attribute, viz. MRR the highest value is taken, for a minimum value-type attribute, viz. TWR and SR, the lowest value.

The respective formulae to obtain normalized experimental results are as follows:

- “Higher-the-better” value:

$$x_{ij} = \frac{y_{ij} - \min_i y_{ij}}{\max_i y_{ij} - \min_i y_{ij}} \quad (\text{Eq 1})$$

- “Lower-the-better” value:

$$x_{ij} = \frac{\max_i y_{ij} - y_{ij}}{\max_i y_{ij} - \min_i y_{ij}} \quad (\text{Eq 2})$$

where y_{ij} is the j th performance characteristic in the i th experiment. Furthermore $\max_i y_{ij}$ and $\min_i y_{ij}$ are the maximum and minimum value of j th performance characteristic for alternative i , respectively. Table 4 shows the normalized results of

experimental results obtained for performance measures by (1) for MRR and (2) for TWR and SR.

4.3 GRC

Normalization creates a new matrix of difference vectors. From this matrix, a GRC is calculated, expressed as:

- GRC

$$\xi_{ij} = \frac{\min_i \min_j |x_j^0 - x_{ij}| + \zeta \max_i \max_j |x_j^0 - x_{ij}|}{|x_j^0 - x_{ij}| + \zeta \max_i \max_j |x_j^0 - x_{ij}|} \quad (\text{Eq 3})$$

x_j^0 is the ideal normalized result for the j th performance characteristic. The row labeled by “ideal” in Table 4 is $x_j^0 = 1$. GRC ξ_{ij} is computed by selecting a proper distinguishing coefficient ζ (in general, $\zeta = 1$) by use of (3).

- GRG

Finally, the GRG is obtained by averaging the GRC corresponding to each performance measures. Thus by applying (4), all GRGs can be computed.

- GRG

$$r_i = \frac{1}{m} \sum_{j=1}^m \xi_{ij} \quad (\text{Eq 4})$$

The GRGs of the set of compared series provide a ranking of the alternatives, where a higher value determines a better alternative. By analysis of the GRG, we can understand which factors will crucially affect reference factors. The GRG computed by averaging the GRC, are used to analyze the relational degree of the multiple performance characteristics (Ref 54). This relationship is hold for any distinguishing coefficient. Also as stated by earlier researchers, Lin and Lin “...the higher GRG represents that the corresponding result is closer to the ideal normalized value (optimal)” (Ref 39).

The GRG obtained for each experimental run and the ranking order of the experiment is shown in Table 5. It is seen

Table 4 Normalization (data pre-processing) of the experimental results for each performance measures

| No. of run Ideal | MRR | | | TWR | | | SR | | |
|---------------------|--------|--------|--------|--------|--------|--------|--------|--------|--------|
| | 1 | 1 | 1 | 1 | 1 | 1 | 1 | 1 | 1 |
| 1 | 0.7368 | 0.5939 | 0.8559 | 0.5556 | 0.5575 | 0.5591 | 0.8472 | 0.8126 | 1.0000 |
| 2 | 0.7826 | 0.6802 | 0.9369 | 0.5896 | 0.5833 | 0.5948 | 0.6561 | 0.8688 | 0.8609 |
| 3 | 0.8344 | 1.0000 | 0.8813 | 0.7219 | 0.6923 | 0.7775 | 0.6615 | 0.5377 | 0.6177 |
| 4 | 0.5833 | 0.7452 | 0.7481 | 0.5379 | 0.5207 | 0.5274 | 0.5605 | 0.6107 | 0.6685 |
| 5 | 0.5833 | 0.5043 | 0.6499 | 0.5556 | 0.5385 | 0.5176 | 0.7832 | 0.5632 | 0.7494 |
| 6 | 0.5122 | 0.6802 | 0.5976 | 0.6651 | 0.6702 | 0.6822 | 0.5489 | 0.5527 | 0.5429 |
| 7 | 0.6774 | 0.5652 | 0.7481 | 0.5896 | 0.5779 | 0.5825 | 0.6616 | 0.6923 | 0.8307 |
| 8 | 0.5228 | 0.6257 | 0.5636 | 0.7804 | 0.7683 | 0.8746 | 0.7756 | 0.8688 | 0.6453 |
| 9 | 0.8344 | 0.5652 | 0.6099 | 1.0000 | 1.0000 | 0.9824 | 0.5645 | 0.5911 | 0.5318 |
| 10 | 0.7368 | 0.7222 | 0.6359 | 0.5844 | 0.5888 | 0.5764 | 0.5955 | 0.5896 | 0.5778 |
| 11 | 0.7159 | 0.7959 | 0.6359 | 0.7297 | 0.7412 | 0.7362 | 0.5767 | 0.5047 | 0.4737 |
| 12 | 0.5019 | 0.5391 | 0.8813 | 0.6054 | 0.5833 | 0.5765 | 0.7910 | 0.8044 | 0.9738 |
| 13 | 1.0000 | 0.8864 | 0.9674 | 0.4737 | 0.4737 | 0.4737 | 0.8720 | 1.0000 | 0.8151 |
| 14 | 0.7368 | 0.5793 | 0.7878 | 0.8709 | 0.8400 | 1.0000 | 0.4736 | 0.5259 | 0.5440 |
| 15 | 0.4737 | 0.4737 | 0.4737 | 0.7714 | 0.6848 | 0.7266 | 0.8625 | 0.5896 | 0.9489 |
| 16 | 0.5339 | 0.6257 | 1.0000 | 0.6853 | 0.6848 | 0.6906 | 1.0000 | 0.7858 | 0.7243 |
| 17 | 0.5972 | 0.5270 | 0.6644 | 0.7219 | 0.7412 | 0.7172 | 0.7151 | 0.8720 | 0.6843 |
| 18 | 0.6269 | 0.5270 | 0.5745 | 0.7377 | 0.7590 | 0.9489 | 0.5366 | 0.4737 | 0.6550 |

Table 5 GRG for each experimental run

| Run no. | GRG | Order |
|---------|--------|-------|
| 1 | 0.7243 | 6 |
| 2 | 0.7282 | 5 |
| 3 | 0.7471 | 3 |
| 4 | 0.6114 | 16 |
| 5 | 0.6050 | 18 |
| 6 | 0.6058 | 17 |
| 7 | 0.6584 | 12 |
| 8 | 0.7139 | 7 |
| 9 | 0.7421 | 4 |
| 10 | 0.6231 | 15 |
| 11 | 0.6567 | 13 |
| 12 | 0.6952 | 9 |
| 13 | 0.7736 | 1 |
| 14 | 0.7065 | 8 |
| 15 | 0.6672 | 11 |
| 16 | 0.7478 | 2 |
| 17 | 0.6934 | 10 |
| 18 | 0.6488 | 14 |

that experiment #13 has the best multiple performance characteristics among the 18 runs performed, having highest relational grade. Hence it is the optimal. It is followed by experiments # 16 and 3, being ranked as second and third, respectively. In other words, optimization of multiple performance characteristics is converted into optimization of a single GRG.

5. Results and Interpretation

Table 6 shows the mean of the GRG for each level of the machining parameters chosen for this study. The orthogonal experiment design separates out the effect of each machining parameter on the GRG at different levels. For example, the mean of GRG for the factor A viz. aspect ratio at levels 1 and 2 can be calculated by taking the average of the GRG for the experiment no. 1-9 and 10-18, respectively (shown in Table 2). Similarly, mean of the GRG for each level of other machining parameters can also be computed. In addition, the total mean of

Table 6 Response table for GRG

| Factor | Machining parameter | Average GRG | | | Max.-min. | Ranking |
|--------|-------------------------------|-------------|---------|---------|-----------|---------|
| | | Level 1 | Level 2 | Level 3 | | |
| A | Aspect ratio | 0.7179 | 0.6541 | ... | 0.0638 | 2 |
| B | Pulse current | 0.6898 | 0.6840 | 0.6844 | 0.0058 | 8 |
| C | Pulse ON time | 0.6890 | 0.6443 | 0.7248 | 0.0804 | 1 |
| D | Duty cycle | 0.6714 | 0.6983 | 0.6884 | 0.0268 | 4 |
| E | Gap voltage | 0.6890 | 0.6747 | 0.6944 | 0.0197 | 7 |
| F | Tool electrode lift time | 0.6703 | 0.6816 | 0.7062 | 0.0359 | 3 |
| G | Abrasive powder concentration | 0.6756 | 0.6853 | 0.6972 | 0.0216 | 6 |
| H | Abrasive particle size | 0.6715 | 0.6944 | 0.6922 | 0.0229 | 5 |

Total mean value of the GRG = 0.68603

the GRG for the 18 experiments is also calculated and listed in Table 6. The total mean value of the GRG is 0.68603.

As stated by Fung, "...the grey relational grade represents the level of co-relation between the reference sequence and the comparability sequence" (Ref 50). The greater value of the GRG means that the comparability sequence has a stronger correlation to the reference sequence. Therefore, the optimal level of the machining parameters is the level with the greatest GRG value. The level value marked asterisks (*) in response table, indicates that they results in a better APM-EDM performance. Based on the GRG given in Table 6, the optimal machining performance for MRR, TWR, and SR was obtained for aspect ratio (level 1), pulse current (level 1), pulse ON time (level 3), duty cycle (level 2), gap voltage (level 3), tool electrode lift time (level 3), abrasive powder concentration (level 3), and abrasive particle size (level 2) combination. Accordingly, the level constitution of optimal machining parameters are A1, B1, C3, D2, E3, F3, G3, and H2 in the case of multiple performance characteristics optimization for APM-EDM, since higher GRG values yield better quality.

The difference between the maximum and the minimum value of the GRG for APM-EDM machining parameters is also calculated and tabulated in Table 6. The tabulated results are follows: 0.0638 for aspect ratio, 0.0058 for pulse current, 0.0804 for pulse ON time, 0.0268 for duty cycle, 0.0197 for gap voltage, 0.0359 for tool electrode lift time, 0.0216 for abrasive powder concentration, and 0.0229 for abrasive particle size, respectively. The most significant factor affecting performance characteristics is determined by comparing these values. This comparison gives the level of significance of the process parameters over the multiple performance characteristics. The most effective controllable factor was the maximum of these values. As per Table 6, the maximum value among the controllable factors is for pulse ON time viz. 0.0804. This higher value indicates that the pulse ON time has the strongest effect on the multiple performance characteristics among the

other machining parameters. Furthermore, the significance of role that every process parameter plays over the multiple performance characteristics can be predicted by examining these values.

The order of importance of the machining parameters to the multiple performance characteristics in the APM-EDM process, in sequence can be ranked as: factor C (pulse ON time), A (aspect ratio), F (tool electrode lift time), D (duty cycle), H (abrasive particle size), G (abrasive powder concentration), E (gap voltage), and B (pulse current). This indicates that the APM-EDM performance was strongly affected by the pulse ON time.

Figure 4 shows the main effects plot (response graph) based on GRG where the dash line indicates the value of the total mean of the GRG (viz. 0.68603). Basically, the larger the GRG, the better is the multiple performance characteristics, since it is closer to the ideal value viz. one. Accordingly A1, B1, C3, D2, E3, F3, G3, and H2 are the optimal level of APM-EDM parameters in the case of multiple performance characteristics. The greater values in Fig. 4 depict the high MRR, low TWR, and SR. However, the relative importance among the process parameters for the multiple performance characteristics still needs to be known so that the optimal combinations of the machining parameter levels can be determined more accurately.

5.1 Analysis of Variance (ANOVA)

The ANOVA investigates which APM-EDM process parameters significantly affect the performance measures. This is revealed by separating the total variability of the GRGs, which is measured by the sum of squared deviations from the total mean of the GRG, into contributions by each process parameter and error. In addition *F* test (or Fisher's test) and *P* value (probability) has also been determined (Ref 55). Table 7 shows the results of ANOVA for multiple performance characteristics. Since there are five *P* values less than 0.05,

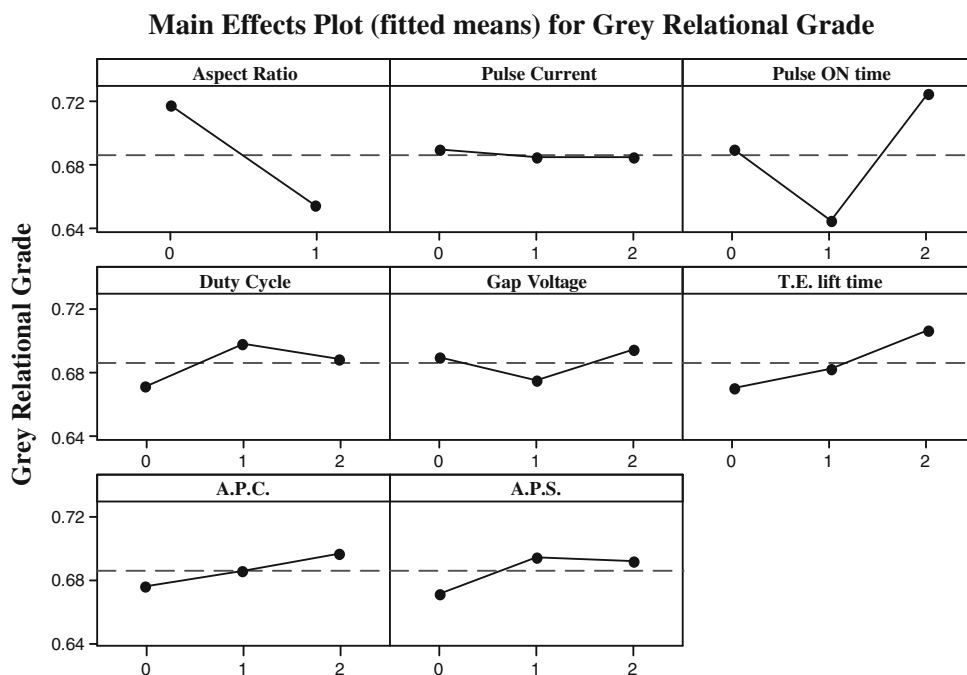


Fig. 4 Effects plot for GRG

Table 7 Results of ANOVA for multiperformance characteristics

| Factor | Machining parameter | Degree of freedom | Sum of square | Mean square | F value | Probability value |
|--------|-------------------------------|-------------------|---------------|-------------|----------|-------------------|
| A | Aspect ratio | 1 | 0.0183106 | 0.0183106 | 408.26** | 0.0024 |
| B | Pulse current | 2 | 0.0001263 | 0.0000632 | 1.41 | 0.4152 |
| C | Pulse ON time | 2 | 0.0194872 | 0.0097436 | 217.25** | 0.0046 |
| D | Duty cycle | 2 | 0.0022100 | 0.00110501 | 24.64** | 0.0390 |
| E | Gap voltage | 2 | 0.0012400 | 0.0006200 | 13.82 | 0.0675 |
| F | Tool electrode lift time | 2 | 0.0040491 | 0.0020246 | 45.14** | 0.0217 |
| G | Abrasive powder concentration | 2 | 0.0014008 | 0.0007004 | 15.62 | 0.0602 |
| H | Abrasive particle size | 2 | 0.0019175 | 0.0009588 | 21.38** | 0.0447 |
| | Error | 2 | 0.0000897 | 0.0000449 | | |
| | Total | 17 | 0.0488313 | | | |

** Significant at 95% CI level

these factors have a statistically significant effect on GRG at the 95.0% confidence interval (CI) level. The results of ANOVA (Table 7) indicate that noise factor-aspect ratio and pulse on time are the most significant process parameters affecting the multiple performance measures. The other factors having significant effects are tool electrode lift time, duty cycle, and abrasive particle size, respectively. Moreover, the other parameters are not significant at 95% confidence interval (CI) level. As per the Table 7, abrasive particle size plays a better role than abrasive particle concentration, during APM-EDM. The finer abrasive particles result in better stock removal rate, which can be attributed to its high particle density and more number of abrasive particles striking the work surface thereby increasing the striking frequency. The increase in the abrasive powder concentration also helps to bridge the gap between the tool electrode and the work material, thus increasing the rate of MRR. This may be attributed to the fact that the bridging effect (formation of powder chain under discharging area) generates multiple discharging effects within a single input pulse, thus increasing frequency of discharging. Thus, the bridging effect between both the electrodes facilitates the dispersion of discharge into several increments, and subsequently increasing MRR (Ref 13, 56). The faster discharging within a single input pulse causes faster erosion of material.

Moreover, it is found that higher abrasive particle concentration with higher particle size display a discharge interference phenomenon. Furthermore, it has also been observed that at higher APC in the dielectric fluid with increased abrasive particle size (APS) results in inter-electrode gap contamination due to the debris and disturbs the discharging between the tool electrode and the work material, eventually leading to abnormal discharges and frequent sorting of the two electrodes, and subsequently low MRR and poor surface finish (Ref 57). Thus, in this study, the highest metal removal depths were achieved at the optimal concentration of SiC (8 g/L). This result is in consonant with the earlier reported results by Chow et al. (Ref 29).

5.2 Confirmation Tests

Once the optimal level of the process parameters is identified, the final step is to predict and validate the improvement of the performance measures using the optimal level. A good indication of the satisfactory experimental runs is

observed by subsequently comparing the results of the confirmation tests with the predicted value. The purpose of the confirmation experiment is to verify the conclusions drawn during the analysis phase.

The estimated γ_m using the optimal levels of the process parameters can be computed by using the following formula:

$$\hat{\gamma} = \gamma_m + \sum_{i=1}^n \hat{\gamma}_i - \gamma_m \quad (\text{Eq 5})$$

where γ_m is the total mean of the GRG, $\hat{\gamma}_i$ is the mean of the GRG at the optimal level, and n is the number of the process parameters that significantly affects the performance characteristics. The confirmation tests were carried out at the optimum levels predicted by the analysis of the results. If the average of confirmation results falls within the range of predicted performance measures as specified confidence interval (CI), the experiments are satisfactory (Ref 58).

From Eq 5, the estimated GRGs using the optimal APM-EDM parameters are computed. Table 8 shows the results of the confirmation tests using the optimal levels of APM-EDM parameters. As noted from Table 8, the MRR is increased from 0.4267 to 0.530 g/min, when the tool wear and SR are minimized from 0.0112 to 0.0096 g/min and from 3.64 to 2.82 μm , respectively. Also, the results of the confirmation tests values as compared to predicted values fall within the 95% CI level. An improvement of 0.2012 (~12%) is noted in GRG, after validation.

6. Conclusions

In this study, the GRA approach, based on the orthogonal experimental design table, is applied to find the optimal machining parameters which minimize the required multiple performance characteristics for APM-EDM of AMCs. The L_{18} ($2^1 \times 3^7$) orthogonal array was selected as experimental plan for the seven control factors namely pulse current (A), pulse ON time (μs), duty cycle (%), gap voltage (V), tool electrode lift time (s), abrasive powder concentration (g/L), abrasive particle size (μm), and a noise factor, aspect ratio (shape of tool electrode). The MRR, TWR, and SR (R_{max}) was adopted to evaluate the machinability performance characteristics.

Table 8 Results of performance measures for initial and optimal process parameters

| | Initial machining parameters | Optimal machining parameters | |
|---------------------------|------------------------------|------------------------------|-------------------------|
| | | Predicted | Experimental |
| Combination level | A2 B3 C2 D1 E2 F3 G1 H3 | A1 B1 C3 D2 E3 F3 G3 H2 | A1 B1 C3 D2 E3 F3 G3 H2 |
| MRR, g/min | 0.4267 | 0.510 | 0.530 |
| TWR, g/min | 0.0112 | 0.0099 | 0.0096 |
| SR, R_a , μm | 3.64 | 2.98 | 2.82 |
| GRG | 0.6167 | 0.7164 | 0.8179 |

Improvement of the GRG = 0.2012

A confirmation test within the optimal machining parameters was conducted to indicate the effectiveness of this proposed approach.

The conclusions of study may be summed up as follows:

The average GRG was obtained through the GRC of each performance characteristic. The largest value of GRG for the APM-EDM parameters was found. On this basis, it is stated that the pulse ON time has the strongest effect among the other process parameters used to study the multiple performance characteristics. The order of importance of the process parameters to the multiple performance characteristics is pulse ON time, aspect ratio, tool electrode lift time, duty cycle, abrasive particle size, abrasive powder concentration, gap voltage, and pulse current.

APM-EDM of AA6061-based MMCs reinforced with 20% alumina (Al_2O_3) particulates with SiC mixed in the dielectric fluid, the optimal level setting of eight process parameters are A1, B1, C3, D2, E3, F3, G3, and H2 for maximizing MRR and minimizing tool wear and SR (R_{max}) according to the results of response table and main effects plot. ANOVA results shows that factor *A* (aspect ratio), factor *C* (pulse ON time), factor *F* (tool electrode lift time), factor *D* (duty cycle), and factor *H* (abrasive particle size) affect the total performance characteristics.

Based on the optimal levels of machining parameters, the confirmation tests yields an increase of MRR from 0.4267 to 0.530 g/min, where as the TWR and the SR (R_{max}) is reduced 0.0112 to 0.0096 g/min and 3.64 to 2.82 μm , respectively.

It can be inferred that the present experiment have shown clearly that the MRR, TWR, and SR in the APM-EDM process can be improved effectively through this proposed approach. This study also indicates that GRA approach could be applied successfully to other operations in which performance measures are determined by many process parameters at multiple quality requests (Ref 43).

As stated by David, "...the GRA, embodies rich philosophical thought of the unity of opposites, such as continuity and discontinuity, quality and quantity, statics and dynamics, etc., in addition to philosophical paradoxical ideas, practical ideas that objects are interrelated, interdependent, and conditioned by each other, such as the analysis of interrelatedness, generation by accumulation, etc (Ref 59)."

Acknowledgments

The authors acknowledge all who have contributed to this article through their research papers, comments, and documents. The authors are extremely grateful and wish special thanks to

Dr. Sachin Maheshwari, Professor & Head (MPAE), NSIT, Dwarka, New Delhi. The authors are also indebted to Prof. P. C. Pandey, Ex-Prof & Head, IIT, Roorkee (India), for being kind enough to provide literature support and words of advice.

References

- V. Kevorkjian, Aluminium-Based Composites, *Adv. Mater. Process.*, 1999, **155**(5), p 27
- A. Ibrahim, F.A. Mohammed, and E.J. Lavernia, Metal Matrix Composites—A Review, *J. Mater. Sci.*, 1991, **26**, p 1137–1156
- J.M. Monaghan, The Use of Quick-Stop Test to Study the Chip Formation of an SiC/Al Metal Matrix Composite and its Matrix Alloy, *Process. Adv. Mater.*, 1994, **4**, p 170
- B. Boardman, *Metal Matrix Composites—An Opportunity for the Off-highway Industry*, SAE International, Toledo, Ohio, 1990
- S. Singh, S. Maheshwari, A. Dey, and P.C. Pandey, Experimental Results and Analysis for Electrical Discharge Machining (EDM) of Aluminium Metal Matrix Composites with Powder-Mixed Dielectric—The Lenth's Method, *Int. J. Manuf. Technol. Manage. (IJMTM), Indersci.*, 2008 (accepted and in press)
- S. Singh, S. Maheshwari, and P.C. Pandey, Optimisation of Multiperformance Characteristics in Electric Discharge Machining of Aluminium Matrix Composites (AMCs) Using Taguchi DOE Methodology, *Int. J. Manuf. Res. (Indersci.)*, 2007, **2**(2), p 138–161
- F. Müller and J. Monaghan, Non-Conventional Machining Of Particle Reinforced Metal Matrix Composite, *Int. J. Mach. Tools Manuf.*, 2000, **40**, p 1351–1366
- J. Perończyk, and J. Kozak, Electrical Discharge Machining (EDM) of the Metal Matrix Composites (MMC), *Proceedings of the VIII International Conference on Rotary Fluid-flow Machines*, Rzeszow–Bystre, Krakow, Poland, 1998, p 391
- R. Dewes, D. Aspinwall, J. Simao, and H.G. Lee, Electrical Discharge Machining and Surface Alloying—The Process, Parameters and State of Play, 2003. <http://www.azom.com/details.asp?ArticleID2082>
- J. Kozak and K.P. Rajurkar, Hybrid Machining Process: Evaluation and Development, *Proceedings of 2nd International Conferences on Machining and Measurement of Sculptured Surfaces*, Krakow, 2001, p 501–536
- S. Singh, S. Maheshwari, and P.C. Pandey, An Experimental Investigation into Abrasive Electrical Discharge Machining (AEDM) of Al_2O_3 Particulate Reinforced Al-Based Metal Matrix Composites, *J. Mech. Eng.*, 2006, **7**(1), p 13–33
- Q.H. Ming and L.Y. He, Powder-Suspension Dielectric Fluid for EDM, *J. Mater. Process. Technol.*, 1995, **52**, p 44–54
- W.S. Zhao, Q.G. Meng, and Z.L. Wang, The Application of Research on Powder Mixed EDM in Rough Machining, *J. Mater. Process. Technol.*, 2002, **129**, p 30–33
- B. Özerkan, and C. Çoğun, Effect of Powder Mixed Dielectric on Machining Performance in Electric Discharge Machining (EDM), *G.U. Journal of Science*, 2005, **18**(2), p 211–228 (ISSN 1303-9709)
- H. Narumiya, N. Mohri, N. Saito, H. Otake, Y. Tsunekawa, T. Takawashi, and K. Kobayashi, EDM by Powder Suspended Working Fluid, *Proceedings of the 9th International Symposium for Electrical Machining*, 1989, p 207–210

16. Y.S. Wong, L.C. Lin, I. Rahuman, and W.M. Tee, Near-Mirror-Finish Phenomenon in EDM Using Powder-Mixed Dielectric, *J. Mater. Process. Technol.*, 1998, **79**, p 30–40
17. K. Furutani, A. Saneto, H. Takezawa, N. Mohri, and H. Miyake, Accretation of Titanium Carbide by Electrical Discharge Machining with Powder Suspended in Working Fluid, *J. Precis. Eng.*, 2001, **25**, p 138–144
18. Y. Uno, A. Okada, T. Yamada, Y. Hayashi, and Y. Tabuchi, Surface Integrity in EDM of Aluminium Bronze with Nickel Powder Mixed Fluid, *J. Jpn. Soc. Electr. Mach. Eng.*, 1998, **32(70)**, p 40–48
19. Y. Uno and A. Okada, Surface Generation Mechanism in Electrical Discharge Machining with Silicon Powder Mixed Fluid, *Int. J. Electro Mach.*, 1997, **2**, p 13–18
20. B.H. Yan and S.L. Chen, Effects of Dielectric with Suspended Aluminium Powder on EDM, *J. Chin. Soc. Mech. Eng.*, 1993, **14(3)**, p 307–312
21. Y.F. Tzeng and C.Y. Lee, Effects of Powder Characteristics on Electro-Discharge Machining Efficiency, *Int. J. Adv. Manuf. Technol.*, 2001, **17(8)**, p 586–592
22. J. Kozak, M. Rozenek, and L. Dabrowski, Study of Electrical Discharge Machining Using Powder-Suspended Working Media, *Proc. Inst. Mech. Eng. B*, 2004, **217**, p 1597–1602
23. C.Y. Lee, “Effects of Powder Characteristics on Electro-Discharge Machining Process,” Master Thesis, Taiwan Chang Gung University, Taiwan (PRC), 1999
24. H. Karafuzi and K. Suda, Study of Electrical Discharge Machining, *Proceedings of 1st All India Machine Tool Design and Research Conference*, Jadavpur, Jadavpur University, India, 1967
25. M.N. Pal, P.K. Mishra, and A. Bhattacharyya, Optimization of Circuit Parameters of A Relaxation Circuit in EDM, *Proceedings of the 4th All India Machine Tool Design and Research (AIMTDR)*, IIT, Madras, India, Conf., V.C. Venkatesh and V. Radhakrishnan, Ed., 1970
26. M.L. Jeswani, Effect of the Addition of Graphite Powder to Kerosene Used as the Dielectric Fluid in Electrical Discharge Machining, *Wear*, 1981, **709**, p 133–139
27. K. Masui, K. Demizu, Y. Sato, and T. Sone, Surface Modification of Tool Steels by Alloying Method Using EDM Process, *Proceedings of ISEM-XI*, 1995, p 419–426
28. A. Erden and S. Bilgin, S. Role of Impurities in Electric Discharge Machining, *Proceedings of the 21st Int. Machining Tools Design and Research Conference*, London, 1980, p 345
29. H.M. Chow, B.H. Yan, F.Y. Huang, and J.C. Hung, Study of Added Powder in Kerosene for the Micro-Slit Machining of Titanium Alloy Using Electro-Discharge Machining, *J. Mater. Process. Technol.*, 2000, **101**, p 95–103
30. M.S. Phadke, *Quality Engineering using Robust Design*, Prentice-Hall, Englewood Cliffs, NJ, 1989
31. S. Singh, S. Maheshwari, and P.C. Pandey, Abrasive Electro-Discharge Machining—An Innovative Technique in Hybrid Machining, *Proceedings of the National Conference on World Class Manufacturing*, AIT, Coimbatore, India, 2003, p 01–06
32. S. Singh, S. Maheshwari, and P.C. Pandey, Analysis of the Abrasive Electro-Discharge Machining (AEDM) for Machining of Advanced Materials. *Proceedings of the National Conference on Recent Developments in Mechanical Engineering*, TIET, Patiala, India, 2003, p 610–614
33. J.L. Deng, Introduction to Grey System Theory, *J. Grey Syst.*, 1989, **1(1)**, p 1–24
34. H. Guo, Identification Coefficient of Grey Relational Grade, *Fuzzy Math. Sp. Issue Grey Syst.*, 1985, **5(2)**, p 55–58 (translated from Chinese)
35. J.L. Deng, Control Problems of Grey Systems, *Syst. Control Lett.*, 1982, **1(5)**, p 288–294
36. J.L. Deng, *The Primary Methods of Grey System Theory*, Huazhong University of Science and Technology Press, Wuhan, 2005
37. C.T. Lin and S.Y. Yang, Selection of Home Mortgage Loans Using Grey Relational Analysis, *J. Grey Syst.*, 1999, **11(4)**, p 359–368
38. W. Hu, B. Hua, and C. Yang, Building Thermal Process Analysis with Grey System Method, *Build. Environ.*, 2002, **37**, p 599–605
39. Lu. Meng, “Modelling and Evaluation of the Effects of Traffic Safety Measures—Comparative Analysis of Driving Assistance Systems and Road Infrastructure,” 2007, Doctoral Thesis submitted to Lund University, SE-22100 Lund, Sweden
40. J.L. Lin and C.L. Lin, The Use of the Orthogonal Array with Grey Relational Analysis to Optimize the Electrical Discharge Machining Process with Multiple Performance Characteristics, *Int. J. Mach. Tools Manuf.*, 2002, **42**, p 237–244
41. C.L. Lin, J.L. Lin, and T.C. Ko, Optimisation of the EDM Process Based on the Orthogonal Array with Fuzzy Logic and Grey Relational Analysis Method, *Int. J. Adv. Manuf. Technol.*, 2002, **19**, p 271–277
42. J.L. Lin and C.L. Lin, The Use of Grey-Fuzzy Logic for the Optimisation of the Manufacturing Process, *J. Mater. Process. Technol.*, 2005, **160**, p 9–14
43. J.T. Huang and Y.S. Liao, Optimisation of Machining Parameters of Wire-EDM Based on Grey Relational Analysis, *Int. J. Prod. Res.*, 2003, **41(8)**, p 1707–1720
44. K.T. Chiang and F.P. Chang, Optimisation of Wire-EDM Process of Particle-Reinforced Material with Multiple Performance Characteristics Using Grey Relational Analysis, *J. Mater. Process. Technol.*, 2006, **180**, p 96–101
45. S.H. Chang, J.R. Hwang, and J.L. Doong, Optimisation of the Injection Molding Process of Short Glass Fiber Reinforced Polycarbonate Composites Using Grey Relational Analysis, *J. Mater. Process. Technol.*, 2000, **97**, p 186–193
46. N. Tosun, Determination of Optimum Parameters for Multiperformance Characteristics in Drilling by Using Grey Relational Analysis, *Int. J. Adv. Manuf. Technol.*, 2005, **28**, p 450–455
47. T. Xue-Rui, L. Yu-Guang, and C. Ming-Zhe, Applications of Grey Relational Analysis in Gastroenterology, *W. J. Gastroenterol.*, 2005, **11(22)**, p 3457–3460
48. T. Xue-Rui and D. Julong, Grey Relational Analysis: A New Statistical Method of Multifactorial Analysis in Medicine, *J. Xi'an Med. Univ. Xi'an China*, 1997, **9**, p 59–65
49. H.H. Chen, P.J. Tsai, S.H. Chen, Y.M. Su, C.C. Chung, and T.C. Huang, Grey Relational Analysis of Dried Roselle (*Hibiscus sabdariffa* L.), *J. Food Process. Preserv.*, 2005, **29**, p 228–245
50. C.P. Fung, Manufacturing Process Optimization for Wear Property of Fibre-Reinforced Polybutylene Terephthalate Composites with Grey Relational Analysis, *Wear*, 2003, **254**, p 298–306
51. K.H. Hsia, M.Y. Chen, and M.C. Chang, Comments on Data Preprocessing for Grey Relational Analysis, *J. Grey Syst.*, 2004, **7(1)**, p 15–20
52. J.L. Deng, *A Course on Grey System Theory*, Huazhong University of Science and Technology Press, Wuhan, 1990
53. J.H. Wu and C.B. Chen, An Alternative Form for Grey Relational Grades, *J. Grey Syst.*, 1999, **11(1)**, p 7–12
54. J.L. Lin and Y.S. Tarn, Optimisation of the Multi-Response Process by the Taguchi Method with Grey Relational Analysis, *J. Grey Syst.*, 1998, **10(4)**, p 355–370
55. R.A. Fisher, *Statistical Methods for Research Workers*, Oliver & Boyd, Edinburgh, 1925
56. S. Singh, S. Maheshwari, A. Dey, and P.C. Pandey, Experimental Results, Analysis for Electrical Discharge Machining (EDM) of Aluminium Metal Matrix Composites With Powder-Mixed Dielectric—The Lenth’s Method, *Int. J. Manuf. Technol. Manage. (IJMTM) (Indersci.)*, 2010, **21(1/2)**, p 67–82
57. P. Pecos and E. Henriques, Influence of silicon powder-mixed dielectric on conventional electrical discharge machining, *Int. J. Mach. Tools Manuf.*, 2003, **43**, p 1465–1471
58. R.K. Roy, *Design of Experiments Using the Taguchi Approach: 16 Steps to Product and Process Improvement*, Wiley-IEEE, New York, 2001
59. D.K.W. Ng, Gray System and Gray Relational Model, *ACM SIGICE Bull.*, 1994, **20(2)**, p 1–9